

# Pion reactions on two-nucleon systems

C. Hanhart

Institut für Kernphysik,  
Forschungszentrum Jülich GmbH, D-52425 Jülich, Germany

## Abstract

We review recent progress in our understanding of elastic and inelastic pion reactions on two nucleon systems from the point of view of effective field theory. The discussion includes  $\pi d$  scattering,  $\gamma d \rightarrow \pi^+ nn$ , and  $NN \rightarrow NN\pi$ . At the end some remarks are made on strangeness production reactions like  $\gamma d \rightarrow K\Lambda N$  and  $NN \rightarrow K\Lambda N$ .

## 1 Introduction

Even after several decades of research, the interactions and dynamics of strongly interacting few-nucleon systems are still not fully understood. Although phenomenological approaches are quite often very successful in describing certain sets of data, a coherent overall picture with clear connection to the fundamental theory, QCD, is still lacking.

The only way to a systematic and well controlled understanding of hadron physics is through the use of an effective field theory. The effective field theory (EFT) for the Standard Model at low energies is chiral perturbation theory (ChPT). This EFT already provided deep insights into strong interaction physics at low energies from systematic studies of the  $\pi\pi$  [1] and the  $\pi N$  [2, 3] system — reviewed in Ref. [4] — as well as the  $NN$  system [5–7]. Here we focus on the field of elastic and inelastic reactions on few nucleon system.

A first step towards a systematic study of elastic and inelastic reactions on nuclei was taken by Weinberg already in 1992 [8]. He suggested that all that needs to be done is to convolute transition operators, calculated perturbatively in standard ChPT, with proper nuclear wave functions to account for the non-perturbative character of the few-nucleon systems. This procedure looks very similar to the so-called distorted wave born approximation used routinely in phenomenological calculations, but, in contrast to this, opens up the possibility

to use a power counting scheme. Within ChPT this idea was already applied to a large number of reactions like  $\pi d \rightarrow \pi d$  [9],  $\gamma d \rightarrow \pi^0 d$  [10, 11],  $\pi^3\text{He} \rightarrow \pi^3\text{He}$  [12],  $\pi^- d \rightarrow \gamma nn$  [13], and  $\gamma d \rightarrow \pi^+ nn$  [14], where only the most recent references were given. We start our presentation with a brief description of  $\pi d$  scattering in sec. 2.

Using standard ChPT especially means to use an expansion in inverse powers of  $M_N$  — the nucleon mass. However, some pion–few-nucleon diagrams employ few–body singularities that lead to contributions non–analytic in  $m_\pi/M_N$ , with  $m_\pi$  for the pion mass [15]. This is discussed in detail in sec. 3. There we show that the appearance of these contributions is linked to the Pauli principle operative while there is a pion in flight. In this context we discuss also the reaction  $\gamma d \rightarrow \pi^+ nn$ , for in the mentioned sense this reaction is complementary to  $\pi d$  scattering. We show that within ChPT the existing data can be described to high accuracy and therefore the reaction qualifies as a tool to measure the  $nn$  scattering length.

A problem was observed when the original scheme by Weinberg was applied to the reactions  $NN \rightarrow NN\pi$  [16, 17]: the inclusion of potentially higher order corrections were large and lead to even larger disagreement between theory and experiment than found in earlier phenomenological studies [18]. For the reaction  $pp \rightarrow pp\pi^0$  one loop diagrams that in the Weinberg counting appear only at NNLO were evaluated [19, 20] and they turned out to give even larger corrections putting into question the convergence of the whole series. However, already quite early the authors of Refs. [21, 22] stressed that an additional new scale enters for  $NN \rightarrow NN\pi$  that needs to be accounted for in the power counting. Since the two nucleons in the initial state need to have sufficiently high kinetic energy to put the pion in the final state on–shell, the initial momentum needs to be larger than

$$p_{thr} = \sqrt{M_N m_\pi} . \quad (1)$$

The proper way to include this scale was presented in Ref. [23] — for a recent review see Ref. [24]. As a result, pion  $p$ -waves are given by tree level diagrams up to NLO and the corresponding calculations showed satisfying agreement with the data. However, for pion  $s$ -waves loops appear already at NLO [23, 25]. In sec. 5 we discuss their effect on the reaction  $NN \rightarrow d\pi$  near threshold. In some detail we will compare the effective field theory result to that on phenomenological calculations.

The central concept to be used in the construction of the transition operators is that of reducibility, for it allows one to disentangle effects of the wave functions and those from the transition operators. As long as the operators

are energy independent, the scheme can be applied straight forwardly [26], however, as we will see below, for energy dependent interactions more care is necessary. This will also be subject of sec. 5.

Once the reaction  $NN \rightarrow d\pi$  is understood within effective field theory one is in the position to also calculate the so-called dispersive and absorptive corrections to the  $\pi d$  scattering length. This calculation will be presented in section 7.

When switching to systems with strangeness one immediately observes that the initial momentum needs to be quite large in any production reaction where there are two nucleons and no strangeness in the initial state. Strangeness conservation demands that at least two particles with strangeness in the final state. Therefore the mass produced is at least

$$\Delta = M_\Lambda - M_N + m_K - m_i ,$$

where  $m_i$  denotes the mass present in the initial state in addition to the two nucleons, e.g.,  $m_i \simeq m_\pi$  for  $\pi d \rightarrow K\Lambda N$  and  $m_i = 0$  for  $NN \rightarrow N\Lambda K$ . Therefore, in the latter reaction the expansion parameter of the ChPT, namely the initial momentum in units of the nucleon mass, is 0.85, using the analog of Eq. (1). Also in the former reaction we are faced with an initial momentum 0.6 in units of the nucleon mass — again not useful as an expansion parameter. Clearly, in those cases the chiral expansion as proposed above is no longer applicable. In sec. 9 we discuss, how for those large momentum transfer reactions the scattering lengths of the outgoing baryons can still be extracted in a controlled way using dispersion theory.

We close with a brief summary and outlook.

## 2 Remarks on the $\pi d$ system

We start our discussion with some remarks on the  $\pi d$  system. Pion-deuteron ( $\pi d$ ) scattering near threshold plays an exceptional role in the quest for the isoscalar  $\pi N$  scattering length  $a_+$ , since the deuteron is an isoscalar target. Therefore one may write  $\text{Re}(a_{\pi d}) = 2a_+ + (\text{few-body corrections})$ . The first term  $\sim a_+$  is simply generated from the impulse approximation (scattering off the proton and off the neutron; diagram (a) of Fig. 1) and is independent of the deuteron structure. Thus, if one is able to calculate the few-body corrections in a controlled way,  $\pi d$  scattering is a prime reaction to extract  $a_+$  (most effectively in combination with an analysis of the high accuracy data on pionic hydrogen). In addition, already at threshold the  $\pi d$  scattering length

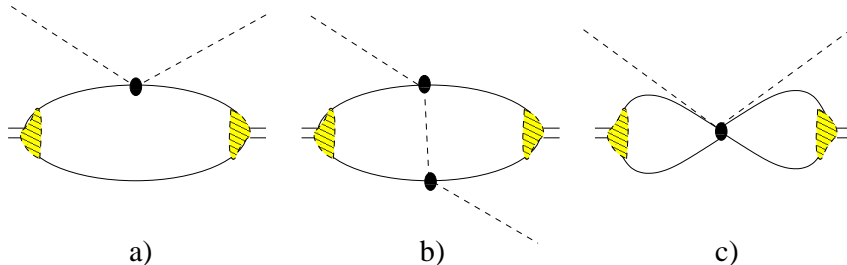


Figure 1: Typical diagrams that contribute to  $\pi d$  scattering. Shown is the one-body term (diagram (a)), the leading two-body correction (diagram (b)) and a possible short-ranged operator (diagram (c)).

is a complex-valued quantity. It is therefore also important to gain a precise understanding of its imaginary part - this issue will be discussed in sec. 7.

Recently the  $\pi d$  scattering length was measured to be [27]

$$a_{\pi d}^{\text{exp}} = (-26.1 \pm 0.5 + i(6.3 \pm 0.7)) \times 10^{-3} m_{\pi}^{-1},$$

where  $m_{\pi}$  denotes the mass of the charged pion. In the near future a new measurement with a projected total uncertainty of 0.5% for the real part and 4% for the imaginary part of the scattering length will be performed at PSI [28]. Clearly, performing calculations up to this accuracy poses a challenge to theory that several groups recently took up [29–34]. In addition, an interesting isospin violating effect in pionic deuterium was found, see [35]. For a review on older work we refer to Ref. [36].

A typical few-body correction to the  $\pi d$  scattering length is shown in diagram (b) of Fig. 1. As we will see below, the contribution of this diagram largely exhausts the value of the  $\pi d$  scattering length not leaving much room for a contribution from  $a_+$ , or stated differently, pointing at a small value of  $a_+$ . Based on calculations within pion less EFT, it was claimed recently that this diagram is sensitive to the short range part of the deuteron wave function [37, 38]. As a consequence field theoretic consistency requires that at the same order there is to be a local operator to absorb this model dependence — the corresponding diagram is shown as diagram (c). Since this diagram comes with an a priori unknown strength not fixed by symmetries,  $\pi d$  scattering would be useless for the extraction of  $a_+$ . However, systematic investigations showed that, as soon as the pion exchange is included explicitly in the  $NN$  potential, diagram (b) can be evaluated in a controlled way [30, 32–34]. Given this we assume from now on that short-ranged operators contributing

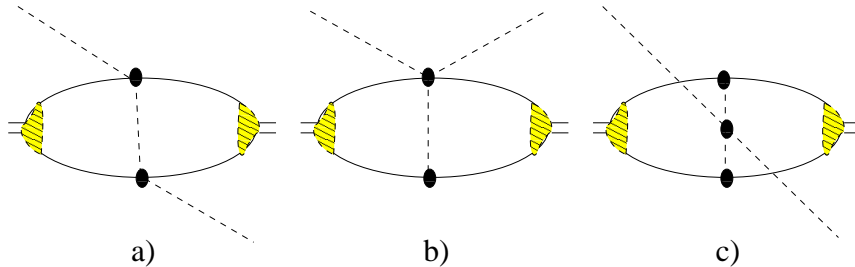


Figure 2: Formally leading few-body corrections to the  $\pi d$  scattering length.

to the  $\pi NN \rightarrow \pi NN$  transition potential scale naturally. In other words, contribute with strength parameters of the order of one. Based on this we may estimate the contribution of diagram (c) of Fig. 1 relative to diagram (b). This kind of analysis gives a relative suppression of the order  $\mathcal{O}(\chi^2)$ , where  $\chi = m_\pi/M_N$  is the standard expansion parameter of ChPT with  $M_N$  ( $m_\pi$ ) for the nucleon (pion) mass. This, together with the knowledge that diagram (a) largely exhausts the value of the  $\pi d$  scattering length, allows us to estimate the theoretical limit for the extraction of  $a_+$  from a measurement of the  $\pi d$  scattering length. We find

$$\Delta a^{\text{theo}} \sim 5 \times 10^{-4} m_\pi^{-1} . \quad (2)$$

To meet this theoretical limit we need to include in the calculation all contributions to the  $\pi d$  scattering length lower than  $\mathcal{O}(\chi^2)$ .

Already in his original work, Weinberg discussed  $\pi d$  scattering at threshold as an illustrative example [8]. As usual, the leading contributions to the transition operators are all those tree-level diagrams that can be constructed from the leading  $\pi N$  and  $\pi\pi$  Lagrangians. Those are shown in Fig. 2. Note that it is very important that the complete set of diagrams is considered, since, for example, both diagram (b) as well as diagram (c) are depending on the particular choice made for the pion field. However, the sum of both is independent of this choice, as was first pointed out in Ref. [39].

Since all diagrams of Fig. 2 contribute to the same chiral order, naively one expects them to give similar contributions. However, explicit numerical evaluations showed, that diagram (a) exceeds the sum of the other two by about two orders of magnitude [8]. Can we understand this? One possible explanation could be that the sum of (b) and (c) is small because of significant cancellations between the two, probably due to the mechanism indicated at the end of the previous paragraph. Another possible explanation was given in

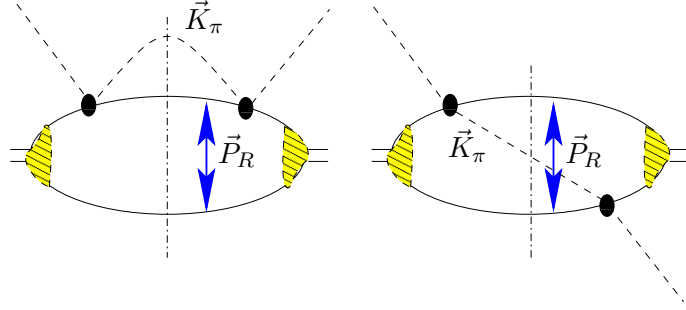


Figure 3: Typical pion loop contributions to  $\pi d$  scattering. Since the exchange of the two nucleons in the intermediate state (at the perpendicular lines) transforms one diagram into the other, the imaginary parts (and their analytic continuation) are linked by the Pauli principle, as described in the text.

Ref. [9]: as a consequence of the small binding energy of the deuteron,  $\epsilon$ , the typical nucleon momentum inside the deuteron,  $\gamma$ , is also small,  $\gamma \sim \sqrt{M_N \epsilon}$ , which turns out to be numerically about 1/3 of the pion mass. Since diagram (a) is proportional to the expectation value of  $1/\bar{q}^2$ , where  $\bar{q}$  denotes the momentum transfer through the pion, and the sum of diagram (b) and (c) is proportional to the expectation value of  $\bar{q}^2/(\bar{q}^2 + m_\pi^2)^2$ , we expect the ratio of the two contributions to be of the order of  $(\gamma/m_\pi)^4 \sim 10^{-2}$ , where  $|\bar{q}|$  was identified with the value of  $\gamma$  defined above. Thus, the small binding energy of the deuteron seems to provide a natural explanation of the relative suppression of diagram (b) + (c) to (a). However, more systematic studies are necessary.

Another important issue is the role of nucleon recoil contributions. All calculations mentioned so far use as starting point the limit of infinitely heavy nucleons; corrections due to the finite nucleon mass are then included as a power expansion in  $1/M_N$ . However, it was already observed in the 70s [40], based on calculations using Gaussian wave-functions, that this way one may miss important terms. This was further investigated in Ref. [15], where the analysis was done model independently and the appearance of these additional contributions was related to the Pauli principle in the intermediate  $NN$  state, while the pion is in flight. This will be discussed in detail in the next section.

### 3 Role of $\pi NN$ cuts

Let us investigate the diagrams of Fig. 3 from the point of view of their  $\pi NN$  cut. Then we may write for the corresponding matrix elements

$$I_{\pi NN}(Q) = \int \frac{dK_\pi K_\pi^2 dP_R P_R^2}{(2\pi)^6} \frac{f(K_\pi^2, P_R^2)}{Q - K_\pi^2/(2m_\pi) - P_R^2/M_N + i0}, \quad (3)$$

where the function  $f$  contains the reaction specific parts like vertex functions, wave functions and transition operators. The only part spelled out explicitly is the  $\pi NN$  propagator, where for simplicity non-relativistic kinematics was chosen. Here  $Q$  denotes the excess energy with respect to the  $\pi NN$  threshold. The goal of this study is to compare the full expression given in Eq. 3 with the corresponding one that emerges when static nucleons are used. This corresponds to taking the limit  $M_N \rightarrow \infty$  prior to integration and we may write

$$I_{\pi NN}^{(static)}(Q) = \int \frac{dK_\pi K_\pi^2 dP_R P_R^2}{(2\pi)^6} \frac{f(K_\pi^2, P_R^2)}{Q - K_\pi^2/(2m_\pi) + i0} + O\left(\frac{m_\pi}{M_N}\right). \quad (4)$$

It was generally assumed that the difference between the integrals of Eqs. (3) and (4) can be accounted for in a polynomial expansion in  $m_\pi/M_N$ . However, this is in general not the case: at pion production threshold  $I_{\pi NN}(Q)$  has a branch point singularity. As we will see this leads to a contribution non-analytic in  $m_\pi/M_N$ , even below pion threshold. To see this, let us study in detail the cut contribution by replacing the  $\pi NN$  propagator by its delta function piece

$$(Q - K_\pi^2/(2m_\pi) - P_R^2/M_N + i0)^{-1} \rightarrow -i\pi\delta(Q - K_\pi^2/(2m_\pi) - P_R^2/M_N).$$

Then we may write

$$I_{\pi NN}^{(cut)}(Q) = -i\pi m_\pi \int \frac{dP_R P_R^2}{(2\pi)^6} f(K_\pi^{on}(Q, P_R^2)^2, P_R^2) K_\pi^{on}(Q, P_R^2).$$

for the full contribution, where  $K_\pi^{on}(Q, P_R^2) = \sqrt{2m_\pi(Q - P_R^2/M_N)}$  and

$$I_{\pi NN}^{(cut,static)}(Q) = -i\pi m_\pi K_\pi^{on}(Q) \int \frac{dP_R P_R^2}{(2\pi)^6} f(K_\pi^{on}(Q)^2, P_R^2)$$

for the static one, with  $K_\pi^{on}(Q)|_{static} = \sqrt{2m_\pi Q}$ . At this point we see already one important difference between the static and the full treatment: while

the imaginary part of the former scales in a completely wrong way, namely according to two-body phase-space, the latter shows the proper scaling as three-body phase space.

But this is not all. Also below the  $\pi NN$  threshold the static contribution gives wrong results. To see this let us focus on the contribution at  $\pi NN$  threshold,  $Q = 0$ . Although for this kinematics both the above integrals are real, the presence of the  $\pi NN$  cut still plays a significant role. To evaluate the relevant integral the on-shell momentum  $K_\pi^{on}(Q, P_R^2)$  needs to be continued analytically to imaginary values using the prescription

$$K_\pi^{on}(0, P_R^2) = \sqrt{-2m_\pi P_R^2/M_N} \rightarrow i\sqrt{2m_\pi P_R^2/M_N} .$$

With this we get

$$I_{\pi NN}^{(cut)}(0) = \pi m_\pi \sqrt{\frac{2m_\pi}{M_N}} \int \frac{dP_R P_R^3}{(2\pi)^6} f(K_\pi^{on}(0, P_R^2)^2, P_R^2) .$$

whereas

$$I_{\pi NN}^{(cut,static)}(0) = 0 .$$

Thus, taking the  $M_N \rightarrow \infty$  limit prior to integration is in general not allowed in the presence of few-body cuts.

The natural question is: when does this matter? As explained the mentioned effect originates from the opening of the physical  $\pi NN$  threshold. However, this threshold can only matter, if the  $\pi NN$  state is allowed by selection rules. In the isospin limit the two nucleons are identical particles that are to obey the Pauli principle. It therefore depends on the operator that acts on the deuteron wave function to produce the intermediate pion, whether or not the  $NN$  state is allowed and, consequently, whether the above contributions matter.

Let us first look at  $\pi d$  scattering. The leading operator that contributes to the  $\pi N \rightarrow \pi N$  transition is the so-called Weinberg-Tomozawa term  $\propto \epsilon^{abc} \tau^c$ , which is a vector in isospin space, but spin and momentum independent. Therefore, this operator acting on the deuteron (isospin 0 and spin 1), leads to an  $NN$  state that is isospin 1 and spin 1, predominantly in an  $s$ -wave due to the momentum independence of the transition operator. This  $NN$  state is forbidden by the Pauli principle and therefore all said in the first part of this section does not matter and the static approximation gives a good description of the leading few-body correction. The same holds, e.g., for  $\pi d \rightarrow \gamma NN$ .

However, there are reactions where we expect the above terms to become significant. One example is the reaction  $\gamma d \rightarrow \pi^+ nn$  that will be discussed



in more detail in the next section. Here the operator acting on the deuteron wave function in leading order is the so-called Kroll–Ruderman term, which is a vector in both isospin as well as spin space. Thus, a transition to an  $NN$  pair in the  $^1S_0$  isovector state, which is allowed by the Pauli principle, is possible. This reaction was studied in detail in Ref. [41], and indeed the pattern sketched above on general grounds was observed. However, for a Pauli allowed intermediate state, the two nucleons will interact. It was found that the inclusion of the two-nucleon intermediate state gives a significant contribution, however, numerically smaller than the static exchange itself. This is different to the case of  $\pi d$  scattering with an isoscalar  $\pi N$  interaction that also leads to a Pauli allowed intermediate state. In this case the inclusion of the  $NN$  interaction at threshold numerically restored the contribution of the static exchange [42].

## 4 The reaction $\gamma d \rightarrow \pi^+ nn$

The reaction  $\gamma d \rightarrow \pi^+ nn$  was studied intensively already in the 70s — for a review see Ref. [43]. At this time only diagrams (a1) and (a2) of Fig. 4 were included. In Ref. [43] there is only one comment to an unpublished work, where pion rescattering (diagrams (c1) and (c2) of Fig. 4) was calculated, however, in the static approximation. It is stated that the inclusion of this contribution destroys the nice agreement of the calculation based on the one-body terms only and therefore it will no longer be considered. Based on the discussion of the previous section we now understand, why the static pion exchange diagram gave a contribution way too large: in a complete calculation it would have been largely canceled by the recoil corrections, since the two-nucleon state in diagrams (b), (c) and (d) can go on-shell while the pion is in flight.

The results of our calculation are shown in Fig. 5. At leading order and next-to-leading order only one-body terms contribute (c.f. Fig. 4) with their strength fixed by the chiral Lagrangian. The relevant  $\gamma p \rightarrow \pi^+ n$  vertices are momentum independent in both cases and therefore their energy dependence is identical. At NNLO there is a counter term for the transition  $\gamma p \rightarrow \pi^+ n$  and the strength of the one-body operator can be adjusted to data [44]. This gives a large fraction of the shift in strength when going from NLO to NNLO. In addition the amplitude gets energy dependent [45]. Another source of energy dependence comes from the few-body corrections as well as higher partial waves that start to contribute at this order. As can be seen from the figure, the data is described very nicely in the whole low energy region considered.

It seems as if the few body corrections, when treated properly, only have

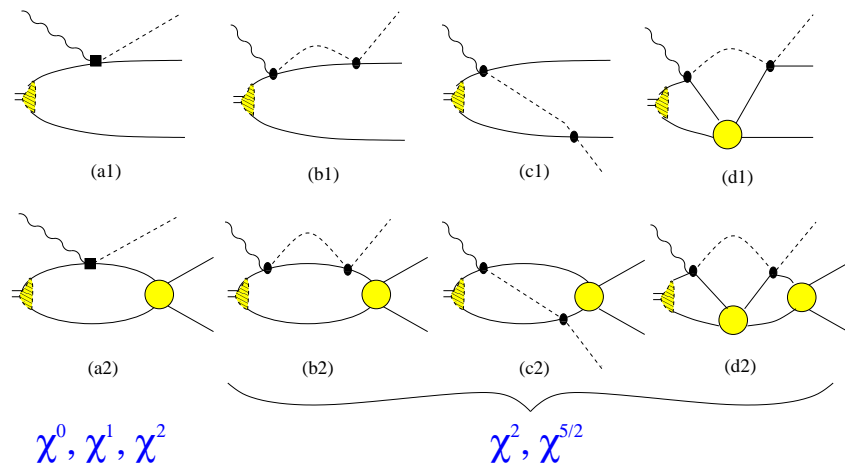


Figure 4: Diagrams contributing to  $\gamma d \rightarrow \pi^+ nn$  up to order  $\chi^{5/2}$ . As before, solid lines denote nucleons, and dashed lines pions. The wavy lines denote photons. The hatched areas denote the deuteron wave function and the filled circles the  $NN$  interaction.

a minor effect on the event rates for  $\gamma d \rightarrow \pi^+ nn$ , however, this is correct only for the total cross section. Especially the neutron momentum distributions are sensitive to higher order corrections and those are to be understood to very high accuracy, in order to make use of this reaction to extract the  $nn$  scattering length.

On the level of neutron momentum distributions diagram (a1) leads to very specific signals due to the so-called quasi-free production. When all particles in the final state go forward, the intermediate proton is very near on-shell and the diagram gives a large contribution, which decreases quickly, however, as we go away from forward kinematics. In addition, the quasi-free production favors large relative momenta of the two neutrons. Near threshold this is clear, as — in the center of mass system — the spectator neutron keeps on going with half the deuteron momentum, whereas the reaction neutron gets decelerated to almost at rest through the production process.

All diagrams with a final-state interaction, on the other hand, give contributions peaked at small relative  $nn$  momenta and almost insensitive to their orientation. This is illustrated in Fig. 6, where the differential rate is shown for two different angles as a function of the relative  $nn$  momentum  $\vec{P}_R$ . The dashed line denotes the distribution where  $\vec{P}_R$  is directed along the beam axis, whereas for the solid line it is perpendicular to the beam. In the former case

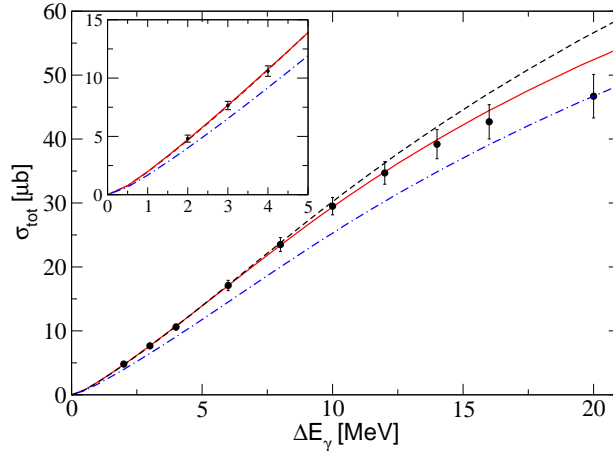


Figure 5: Total cross section of the reaction  $\gamma d \rightarrow \pi^+ nn$  at LO (dashed line), NLO (dash-dotted line) and  $\chi^{5/2}$  order (solid line) together with experimental data from Ref. [46].

the distribution shows a clear two-peak structure — the quasi-free production shows up at large  $P_R$  and the final state peak shows up at small  $P_R$ . In the latter case, on the other hand, the quasi free contribution has disappeared and only the final state interaction piece remains with basically identical strength.

The height and shape of the FSI peak is sensitive to the value of  $a_{nn}$  — the neutron-neutron scattering length. A systematic study revealed that high accuracy data on  $\gamma d \rightarrow \pi^+ nn$  will allow one to extract the  $nn$  scattering length with an uncertainty of the order of 0.1 fm which is compatible with that estimated for the competing reactions,  $pd \rightarrow nnp$  [47] and  $\pi^- d \rightarrow \gamma nn$  [13].

## 5 $NN \rightarrow d\pi$

As sketched in the introduction, for reactions of the type  $NN \rightarrow NN\pi$  a simultaneous expansion in the large initial momentum  $p_{\text{thr}} \sim \sqrt{m_\pi M_N}$ , that also sets the scale for the typical momenta in the loops, and the pion mass is compulsory. Before we go into details in discussing a particular reaction channel we would like to briefly illustrate the impact of this. In practice this means that momenta and pion masses are to be treated independently in the power counting.

To see how this works let us for example estimate the contributions of the

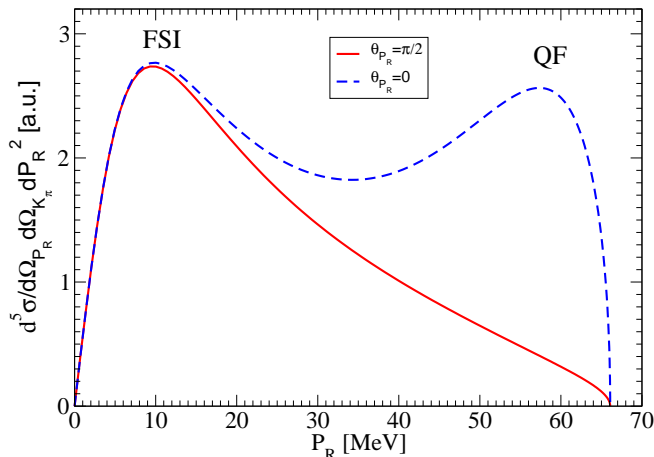


Figure 6: Predicted event rate for the reaction  $\gamma d \rightarrow \pi^+ nn$  at an excitation energy of 5 MeV as a function of the  $nn$  relative momentum  $P_R$  for two different orientations of it. The region of small values of  $P_R$  are dominated by the  $nn$  final state interaction (FSI) and that of large values of it by the quasi-free production (QF).

loops shown in Fig. 7. For diagram (a) we then estimate

$$\frac{p}{f_\pi^2} \left( \frac{p}{f_\pi} \right)^3 \left( \frac{1}{p^2} \right)^2 \left( \frac{1}{p} \right)^2 \frac{p^4}{(4\pi)^2} \sim \frac{p^2}{M_N^2},$$

where the different terms refer to the  $\pi N \rightarrow \pi N$  vertex, the three  $\pi NN$  vertices, the two pion propagators, the two nucleon propagators, and the integral measure, in order. Each individual piece was expressed by the dimensionful parts, where momenta were identified with their typical values. For more details we refer to Appendix E of Ref. [24]. To come to the order estimate we used  $4\pi f_\pi \sim M_N$  and dropped an overall factor of  $1/f_\pi^3$  common to all production amplitudes. On the other hand we find for diagram (b)

$$\left\{ \left( \frac{m_\pi}{f_\pi} \right)^2 \frac{1}{m_\pi} \frac{1}{m_\pi^2} \frac{m_\pi^4}{(4\pi)^2} \right\} \frac{1}{p^2} \left( \frac{p}{f_\pi} \right) \sim \frac{m_\pi^3}{p M_N^2}.$$

The expression in the curly bracket refers to the pion loop — it contains two  $\pi N \rightarrow \pi N$  vertices, one nucleon and one pion propagator as well as the integral measure — however, in this case the typical momentum is of the order of  $m_\pi$  instead of  $p_{\text{thr}}$  as in the previous example. The reason is simply that one may

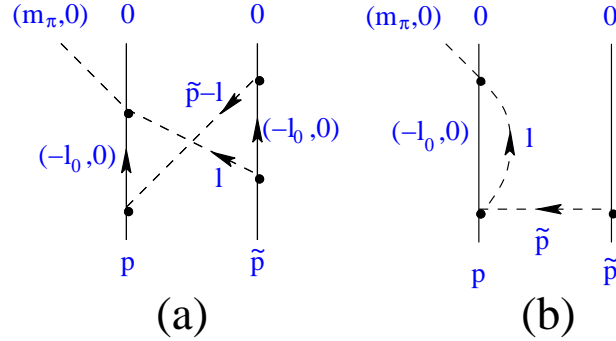


Figure 7: Two typical pion loops that contribute to  $NN \rightarrow NN\pi^+$ . Diagram (a) starts to contribute at NLO whereas diagram (b) starts to contribute at  $N^4\text{LO}$ .

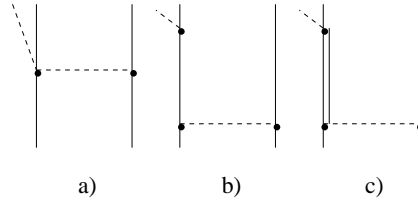


Figure 8: Tree level diagrams that contribute to  $pp \rightarrow d\pi^+$  up to NLO. Solid lines denote nucleons, dashed ones pions and the double line the propagation of a Delta-isobar.

choose in the loop the momenta such that the large momentum does not run through the pion. Then the large scale does not appear in the loop at all since the leading heavy baryon propagator feels energies only. Outside the curly bracket the momentum transfer is large and therefore the pion propagator as well as the pion vertex appear with  $p \sim p_{\text{thr}}$ .

If we compare the two order assignments we observe that under the assumption that momenta are of order  $m_\pi$ , both expressions appear at the same order and are therefore expected to be of similar order of magnitude. However, if we assume  $p$  to be of order  $p_{\text{thr}}$ , then diagram (a) is of order  $m_\pi/M_N$  and diagram (b) is of order  $(m_\pi/M_N)^{5/2}$ , which corresponds to a relative suppression of  $(m_\pi/M_N)^{3/2} \sim 1/20$ . An explicit calculation [19] revealed an even larger suppression of diagram (b), which turned out to be suppressed by a factor of 50 compared to (a). For more examples we refer to Ref. [24].

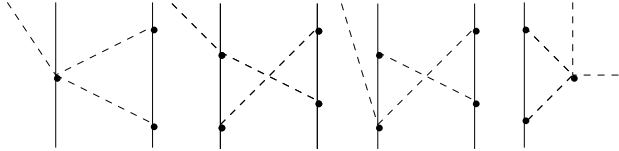


Figure 9: Irreducible pion loops with nucleons only that start to contribute to  $NN \rightarrow NN\pi$  at NLO that were considered in Ref. [25].

As already discussed in the context of  $\pi d$  scattering, in some cases only the sum of various diagrams can give meaningful results, since the individual diagrams depend on the choice made for the pion field. Due to the reordering of loop diagrams, the members of those invariant subgroups are not necessarily of the same chiral order anymore, in contrast to the original Weinberg counting. That, regardless this, also the new scheme gives meaningful results is demonstrated in Ref. [48].

The tree level amplitudes that contribute to  $pp \rightarrow d\pi^+$  are shown in Fig. 8. In Ref. [25] all NLO contributions of loops that start to contribute to  $NN \rightarrow NN\pi$  at NLO were<sup>1</sup> calculated in threshold kinematics — that is neglecting the distortions from the  $NN$  final- and initial state interaction and putting all final states at rest. At threshold only two amplitudes contribute, namely the one with the nucleon pair in the final and initial state in isospin 1 (measured, e.g., in  $pp \rightarrow pp\pi^0$ ) and the one where the total  $NN$  isospin is changed from 1 to 0 (measured, e.g., in  $pp \rightarrow d\pi^+$ ). It was found that the sum all loops that contain  $\Delta$ -excitations vanish in both channels. This was understood, since the loops were divergent and at NLO no counter term is allowed by chiral symmetry. On the other hand the nucleonic loops were individually finite. It was found that the sum of all nucleonic loops that contribute to  $pp \rightarrow pp\pi^0$  vanish, whereas the sum of those that contribute to  $pp \rightarrow d\pi^+$  gave a finite answer. The resulting amplitude grows linear with the initial momentum. In Ref. [49] it was pointed out that this growth of the amplitude is problematic: when evaluated for finite outgoing  $NN$  momenta, the transition amplitudes turned out to scale as the momentum transfer. Especially, the amplitudes then grew linearly with the external  $NN$  momenta. As a consequence, once convoluted with the  $NN$  wave functions, a large sensitivity to those was found, in conflict with general requirements from field theory. The solution to this puzzle was presented in Ref. [50] and will be reported now.

---

<sup>1</sup>In a scheme with two expansion parameters — here  $m_\pi$  and  $p_{thr}$  — loops no longer contribute at a single order but at all orders higher than where they start to contribute.

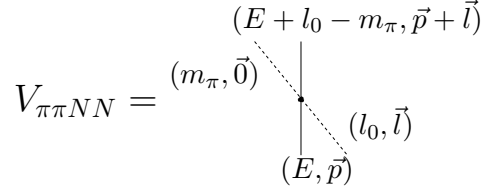


Figure 10: The  $\pi N \rightarrow \pi N$  transition vertex: definition of kinematic variables as used in the text.

The observation central to the analysis is that the leading  $\pi N \rightarrow \pi N$  transition vertex, as it appears in Fig. 8a, is energy dependent. Using the notation of Fig. 10 its momentum and energy dependent part may be written as [2]

$$\begin{aligned}
 V_{\pi\pi NN} &= l_0 + m_\pi - \frac{\vec{l} \cdot (2\vec{p} + \vec{l})}{2M_N} \\
 &= \underbrace{2m_\pi}_{\text{on-shell}} + \underbrace{\left( l_0 - m_\pi + E - \frac{(\vec{l} + \vec{p})^2}{2M_N} \right)}_{(E' - H_0) = (S')^{-1}} - \underbrace{\left( E - \frac{\vec{p}^2}{2M_N} \right)}_{(E - H_0) = S^{-1}}. \quad (5)
 \end{aligned}$$

For simplicity we skipped the isospin part of the amplitude. The first term in the last line denotes the transition in on-shell kinematics, the second the inverse of the outgoing nucleon propagator and third the inverse of the incoming nucleon propagator. First of all we observe that for on-shell incoming and outgoing nucleons, the  $\pi N \rightarrow \pi N$  transition vertex takes its on-shell value  $2m_\pi$  — even if the incoming pion is off-shell, as it is for diagram (a) of Fig. 8. This is in contrast to standard phenomenological treatments [51], where  $l_0$  was identified with  $m_\pi/2$  — the energy transfer in on-shell kinematics — and the recoil terms were not considered. Note, since  $p_{thr}^2/M_N = m_\pi$  the recoil terms are to be kept.

A second consequence of Eq. (5) is even more interesting: when the  $\pi N \rightarrow \pi N$  vertex gets convoluted with  $NN$  wave functions, only the first term leads to a reducible diagram. The second and third term, however, lead to irreducible contributions, since one of the nucleon propagators gets canceled. This is illustrated in Fig. 11, where those induced topologies are shown that appear, when one of the nucleon propagators is canceled (marked by the filled box) in the convolution of typical diagrams of the  $NN$  potential with the  $NN \rightarrow NN\pi$  transition operator. Power counting gives that diagram (b) and (c) appear only at order  $N^4\text{LO}$  and  $N^3\text{LO}$ , respectively. However, diagram (a)

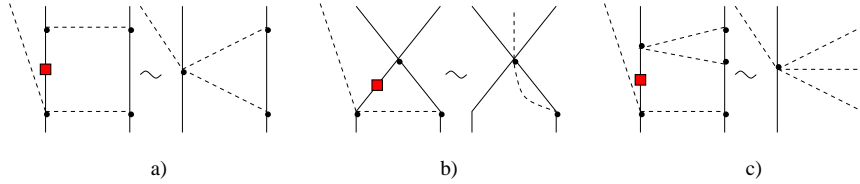


Figure 11: Induced irreducible topologies, when the off-shell terms of Eq. (5) hit the  $NN$  potential in the final state. The filled box on the nucleon line denotes the propagator canceled by the off-shell part of the vertex.

starts to contribute at NLO and it was found in Ref. [50] that those induced irreducible contributions cancel the finite remainder of the NLO loops in the  $pp \rightarrow d\pi^+$  channel. Thus, up to NLO only the diagrams of Fig. 8 contribute to  $pp \rightarrow d\pi^+$ , with the rule that the  $\pi N \rightarrow \pi N$  vertex is put on-shell.

The result found in Ref. [50] is shown in Fig. 12 as the solid line, where the total cross section (normalized by the energy dependence of phase space) is plotted against the normalized pion momentum. The dashed line is the result of the model by Koltun and Reitan [51], as described above. The data sets are from TRIUMF [52], IUCF [53], and COSY [54].

## 6 Comparison to phenomenological works

All recent phenomenological calculations for  $NN \rightarrow NN\pi$  add additional diagrams to the model of Ref. [51]. Here we will focus only on  $pp \rightarrow d\pi^+$ . Phenomenological calculations for this reaction in near threshold kinematics are given, e.g., in Ref. [55] and Ref. [56]. In both works in addition to the diagrams of Ref. [51] some  $\Delta$ -loops as well as additional short range contributions are included — heavy meson exchanges for the former and off-shell  $\pi N$  scattering<sup>2</sup> for the latter. Based on this the cross section for  $pp \rightarrow d\pi^+$  is overestimated near threshold. How can we interpret this discrepancy in light of the discussion above?

First of all, the NLO parts of the  $\Delta$ -loops cancel, as was shown already in Ref. [25]. However, in both Refs. [55, 56] only one of these diagrams was included and, especially for Ref. [55], gave a significant contribution. In addition, in the effective field theory short ranged operators start to contribute only at N<sup>2</sup>LO. The only diagram of those NLO loops shown in Fig. 9 that is

<sup>2</sup>That those are also short range contributions is discussed in Ref. [24].



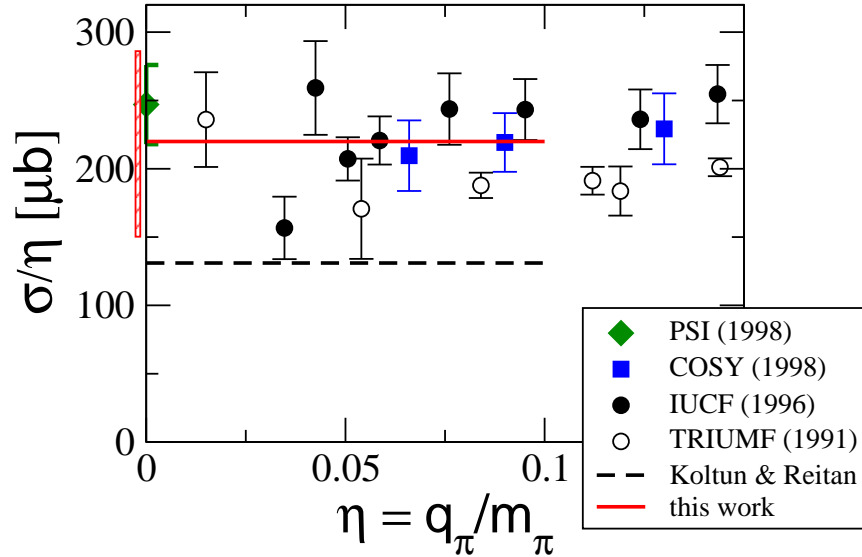


Figure 12: Comparison of the results of Ref. [50] to experimental data for  $NN \rightarrow d\pi$ . The dashed line corresponds to the model of Koltun and Reitan [51], whereas the solid line is the result of the ChPT calculation of Ref. [50]. The estimated theoretical uncertainty (see text) is illustrated by the narrow box. The data is from Refs. [52] (open circles), [53] (filled circles) and [54] (filled squares). The first data set shows twice the cross section for  $pn \rightarrow d\pi^0$  and the other two the cross section for  $pp \rightarrow d\pi^+$ .

effectively included in Ref. [56] is the fourth, since the pion loop there can be regarded as part of the  $\pi N \rightarrow \pi N$  transition  $T$ -matrix. However, as described, the contribution of this diagram gets canceled by the others shown in Fig. 9 and the induced irreducible pieces described above. Therefore, the physics that enhances the cross section compared to the work of Ref. [51] in Refs. [55, 56] is completely different to that of Ref. [50]. However, only the last one is field theoretically consistent as explained in the previous section.

The natural question that arises is that for observable consequences. As explained, in the effective field theory calculation the near threshold cross section for  $pp \rightarrow d\pi^+$  is basically given by a long-ranged pion exchange diagram, whereas the phenomenological calculations rely on short ranged operators with respect to the  $NN$  system. Obviously those observables are sensitive to this difference that get prominent contributions from higher partial waves in the final  $NN$  system. We therefore need to look at the reaction  $pp \rightarrow pn\pi^+$ . Un-

fortunately, the total cross section for this reaction is largely saturated by  $NN$   $S$ -waves in the final state (see, e.g., Fig. 17 in Ref. [24]). On the other hand, linear combinations of double polarization observables allow one to remove the prominent components and the sub-leading amplitudes should be visible. We therefore expect from the above considerations that the phenomenological calculations give good results for polarization observables for  $pp \rightarrow d\pi^+$ , whereas there should be deviations for some of those for  $pp \rightarrow pn\pi^+$ . Predictions for these observables were presented in Ref. [57] and indeed the  $\pi^+$  observables with the deuteron in the final state, reported in Ref. [58], are described well whereas there are discrepancies for the  $pn$  final state (see Fig. 24 of Ref. [24]). For the corresponding data see Ref. [59].

It remains to be seen how well the same data can be described in the effective field theory framework. Up to NNLO the number of counter terms is quite low: there are two counter terms for pion  $s$ -waves, that can be arranged to contribute to  $pp \rightarrow pp\pi^0$  and  $pp \rightarrow d\pi^+$  individually, and then there is one counter term for pion  $p$ -waves, that contributes only to a small amplitude in charged pion production [23]. On the other hand there is a huge amount of even double polarized data available [58–60] — and there is more to come especially for  $pn \rightarrow pp\pi^-$  [61].

## 7 Dispersive corrections to $a_{\pi d}$

Let us come back to  $\pi d$  scattering at threshold. The corresponding scattering length was presented in Eq. (2). In the introductory sections we exclusively focused on the real part. However, now we are in the position to also discuss the imaginary part, which is closely linked to the reaction  $NN \rightarrow d\pi$  through unitarity and detailed balance. One may write

$$4\pi\text{Im}(a_{\pi d}) = \lim_{q \rightarrow 0} q \{ \sigma(\pi d \rightarrow NN) + \sigma(\pi d \rightarrow \gamma NN) \} , \quad (6)$$

where  $q$  denotes the relative momentum of the initial  $\pi d$  pair. The ratio  $R = \lim_{q \rightarrow 0} (\sigma(\pi d \rightarrow NN) / \sigma(\pi d \rightarrow \gamma NN))$  was measured to be  $2.83 \pm 0.04$  [62]. At low energies diagrams that lead to a sizable imaginary part of some amplitude are expected to also contribute significantly to its real part. Those contributions are called dispersive corrections. As a first estimate Brückner speculated that the real and imaginary part of these contributions should be of the same order of magnitude [63]. This expectation was confirmed within Faddeev calculations in Refs. [64]. Given the high accuracy of the measurement and the size of the imaginary part of the scattering length, another critical

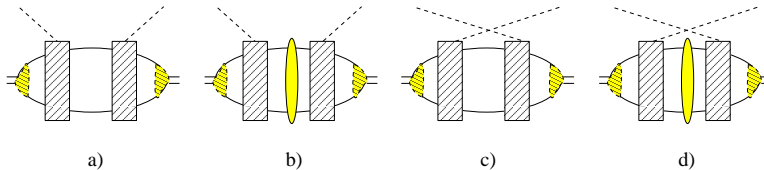


Figure 13: Dispersive corrections to the  $\pi d$  scattering length.

look at this result is called for as already stressed in Refs. [65, 66]. A consistent calculation is only possible within a well defined effective field theory — the first calculation of this kind was presented in Ref. [67] and is briefly sketched here.

To identify the diagrams that are to contribute we first need to specify what we mean by a dispersive correction. We define dispersive corrections as contributions from diagrams with an intermediate state that contains only nucleons, photons and at most real pions. Therefore, all the diagrams shown in Fig. 13 are included in our work. On the other hand, all diagrams that, e.g., have Delta excitations in the intermediate state do not qualify as dispersive corrections, although they might give significant contributions [31].

The hatched blocks in the diagrams of Fig. 13 refer to the relevant transition operators for the reaction  $NN \rightarrow NN\pi$  depicted in Fig. 8. Also in the kinematics of relevance here the  $\pi N \rightarrow \pi N$  transitions are to be taken with their on-shell value  $2m_\pi$ . Using the CD-Bonn potential [68] for the  $NN$  distortions we found for the dispersive correction from the purely hadronic transition

$$a_{\pi d}^{disp} = (-6.3 + 2 + 3.1 - 0.4) \times 10^{-3} m_\pi^{-1} = -1.6 \times 10^{-3} m_\pi^{-1}, \quad (7)$$

where the numbers in the first bracket are the individual results for the diagrams shown in Fig. 13, in order. Note that the diagrams with intermediate  $NN$  interactions and the crossed ones (diagram (c) and (d)), neither of them included in most of the previous calculations, give significant contributions. The latter finding might come as a surprise on the first glance, however, please recall that in the chiral limit all four diagrams of Fig. 13 are kinematically identical and chiral perturbation theory is a systematic expansion around exactly this point. Thus, as a result we find that the dispersive corrections to the  $\pi d$  scattering length are of the order of 6 % of the real part of the scattering length. This number is fully in line with the expectations from power counting, which predicted a relative suppression of the dispersive corrections compared to the leading double scattering term — diagram (b) of Fig. 1 —

of the order of  $(m_\pi/M_N)^{3/2} \sim 5\%$ . Note that the same calculation gave very nice agreement for the corresponding imaginary part [67].

In Ref. [67] also the electro-magnetic contribution to the dispersive correction was calculated. It turned out that the contribution to the real part was tiny —  $-0.1 \times 10^{-3} m_\pi^{-1}$  — while the sizable experimental value for the imaginary part (c.f. Eqs. (2) and 6) was described well.

To get a reliable estimate of the uncertainty of the calculation just presented a NNLO calculation is necessary. At that order a counter term appears for pions at rest that can be fixed from  $NN \rightarrow NN\pi$ , as indicated above. For now we can only present a conservative estimate for the uncertainty by using the uncertainty of order  $2m_\pi/M_N$  one has for, e.g., the sum of all direct diagrams to derive a  $\Delta a_{\pi d}^{disp}$  of around  $1.4 \times 10^{-3} m_\pi^{-1}$ , which corresponds to about 6% of  $\text{Re}(a_{\pi d}^{\text{exp}})$ . However, given that the operators that contribute to both direct and crossed diagrams are almost the same and that part of the mentioned cancellations is a direct consequence of kinematics, this number for  $\Delta a_{\pi d}^{disp}$  is probably too large.

In Ref. [67] a detailed comparison to previous works is given. Differences in the values found for the dispersive corrections were traced to the incomplete sets of diagrams included in those phenomenological studies.

## 8 Summary and Outlook for pion reactions

In the lectures recent progress in our understanding of elastic and inelastic pion reactions on the two-nucleon system was presented. The central reaction discussed was  $\pi d$  scattering at threshold. Arguments were given that in the years to come one should be able to calculate the  $\pi d$  scattering length with sufficient accuracy to use the reaction as one of the prime sources for the isoscalar scattering length  $a_+$ . To reach this not only significant progress was necessary for the coherent  $\pi d$  scattering but also the reactions  $NN \rightarrow NN\pi$  need to be understood. In the future also the role of isospin violation on  $\pi d$  scattering needs to be investigated further as stressed in Ref. [35].

The process  $NN \rightarrow NN\pi$  is a puzzle already since more than a decade. Given the progress presented above we have now reason to believe that this puzzle will be solved soon. This mentioned results could only be found, because a consistent effective field theory was used. For example, the potential problem with the transition operators of Ref. [25], pointed at in Ref. [49], would always be hidden in phenomenological calculations, since the form factors routinely used there always lead to finite, well behaved amplitudes. The very large number of observables available for the reactions  $NN \rightarrow NN\pi$  will provide a

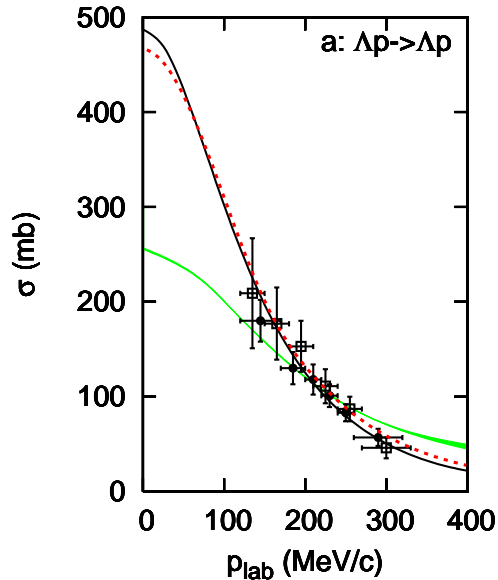


Figure 14: Comparison of different variants for the  $\Lambda N$  interaction to the available data at low energies. The solid line, dashed line, and the light area are the results of Refs. [77–79], in order. The data are from Refs. [75, 76].

non-trivial test to the approach described.

Once the scheme is established, the same field theory can be used to analyze the isospin violating observables measured in  $pn \rightarrow d\pi^0$  [69] and  $dd \rightarrow \alpha\pi^0$  [70]. First steps in this direction were already done in Ref. [71] for the former and in Refs. [72, 73] for the latter.

In the lectures also the reaction  $\gamma d \rightarrow \pi^+ nn$  was discussed. Not only gave those studies a further confirmation that we understand the few body dynamics well within ChPT, but it also promises to become an ideal reaction for the extraction of the  $nn$  scattering length with high accuracy. The corresponding measurements could be performed at HIGS [74].

## 9 Some remarks on strangeness production

As described in the previous sections a lot is already known about the properties and dynamics of systems composed of light quarks only. However, much less is known about the scattering of systems with strangeness, especially for low energies. The reason is of experimental nature: the lifetime of particles

with strangeness is typically too short to allow for secondary scatterings at low energies, necessary to get information on low energy scattering.

Here we will focus on the hyperon–nucleon ( $YN$ ) system. The poor status of our information on the  $YN$  interaction is most obviously reflected in the present knowledge of the  $\Lambda N$  scattering lengths. Attempts in the 1960’s to pin down the low energy parameters for the  $S$ -waves led to results that were afflicted by rather large uncertainties [75, 76]. In Ref. [76] the following values are given for the singlet scattering length  $a_s$  and the triplet scattering length  $a_t$

$$a_s = -1.8 \begin{cases} +2.3 \\ -4.2 \end{cases} \text{ fm and } a_t = -1.6 \begin{cases} +1.1 \\ -0.8 \end{cases} \text{ fm}, \quad (8)$$

where the errors are strongly correlated. The situation of the corresponding effective ranges is even worse: for both spin states values between 0 and 16 fm are allowed by the data. Later, the application of microscopic models for the extrapolation of the data to the threshold, was hardly more successful to pin down the low energy parameters. For example, in Ref. [77] one can find six different models that equally well describe the available data but whose ( $S$ -wave) scattering lengths range from -0.7 to -2.6 fm in the singlet channel and from -1.7 to -2.15 fm in the triplet channel. To illustrate this point in Fig. 14 we show a comparison of model f of Ref. [77] (dark solid line), the Jülich ’04 model [78] (dashed curve), and the result from the recent effective field theory approach of Ref. [79] to the world data.

The natural alternative to scattering experiments are production reactions. However, the central insights of the previous sections were that only within a consistent field theory reliable calculations can be performed for the reactions under considerations. On the other hand, as stressed in the introduction, any strangeness production reaction involves momenta that do not allow for an expansion along the lines just discussed, since the corresponding expansion parameter in this case would be larger than  $1/2$ . Does this mean that one can learn nothing from a study of strangeness production off two nucleon systems?

Not at all. For one thing, an investigation of baryon and meson resonances does not need any detailed knowledge on the production mechanism — most of the relevant information is contained in the Dalitz plots — and the comment of the previous paragraph applies only to this part. But one can learn even more from the production reactions by using that the momentum transfer in those reactions are large. Since this leads to an effectively point-like production operator, one may employ dispersion theory to relate invariant mass spectra of production reactions to elastic scattering data. Obviously, for this no knowledge on the production operator is necessary whatsoever. Then, in

contrast to above, one works with the typical outgoing relative momentum in units of the momentum transfer as expansion parameter.

In the remainder of this text I will only focus on how to extract scattering parameters from production reactions. One aspect of spectroscopy, also discussed in the lectures, namely that of scalar mesons, was described in the recent conference proceeding [80] in very much detail and it will not be repeated here.

The use of dispersion theory was very common in the 50s and the basis for the study to be described now was worked out already then [81]. A controlled method of extraction of scattering lengths from production reactions opens up the opportunity to measure scattering parameters also for unstable states. As an example we will discuss the option to measure the  $\Lambda N$  scattering lengths from  $NN \rightarrow K\Lambda N$  and  $\gamma d \rightarrow K\Lambda N$ . In Refs. [82–84] it was shown, how to derive an integral representation of the scattering length of a pair of outgoing particles (here we show the formula relevant for neutral final states, as is relevant for  $\Lambda N$ ; in the presence of Coulomb interactions the equation has to be modified — see Ref. [83]):

$$a_S = \lim_{m^2 \rightarrow m_0^2} \frac{1}{2\pi} \left( \frac{m_\Lambda + m_N}{\sqrt{m_\Lambda m_N}} \right) \mathbf{P} \int_{m_0^2}^{m_{max}^2} dm'^2 \sqrt{\frac{m_{max}^2 - m^2}{m_{max}^2 - m'^2}} \times \frac{1}{\sqrt{m'^2 - m_0^2} (m'^2 - m^2)} \log \left\{ \frac{1}{p'} \left( \frac{d^2 \sigma_S}{dm'^2 dt} \right) \right\}, \quad (9)$$

where  $\sigma_S$  denotes the spin cross section for the production of a  $\Lambda$ -nucleon pair with invariant mass  $m'^2$ —corresponding to a relative momentum  $p'$ —and total spin  $S$ . In addition  $t = (p_1 - p_{K^+})^2$ , with  $p_1$  being the beam momentum,  $m_0^2 = (m_\Lambda + m_N)^2$ , where  $m_\Lambda$  ( $m_N$ ) denotes the mass of the Lambda hyperon (nucleon), and  $m_{max}$  is some suitably chosen cutoff in the mass integration. In Ref. [82] it was shown that it is sufficient to include relative energies of the final  $\Lambda N$  system of at most 40 MeV in the range of integration to get accurate results.  $\mathbf{P}$  denotes that the principal value of the integral is to be used and the limit has to be taken from above.

The formula as given is applicable if there are no significant effects from crossed channels — this can be monitored by a Dalitz plot analysis — and only a single partial wave contributes. With respect to the angular momentum this can be achieved by a proper choice of  $m_{max}$ . In order to select a single spin state for the outgoing two-particle system polarization observables are necessary. In Refs. [82, 84] the relevant observables are identified for the reactions  $NN \rightarrow NKY$  and  $\gamma d \rightarrow K\Lambda N$ , respectively. The former class of

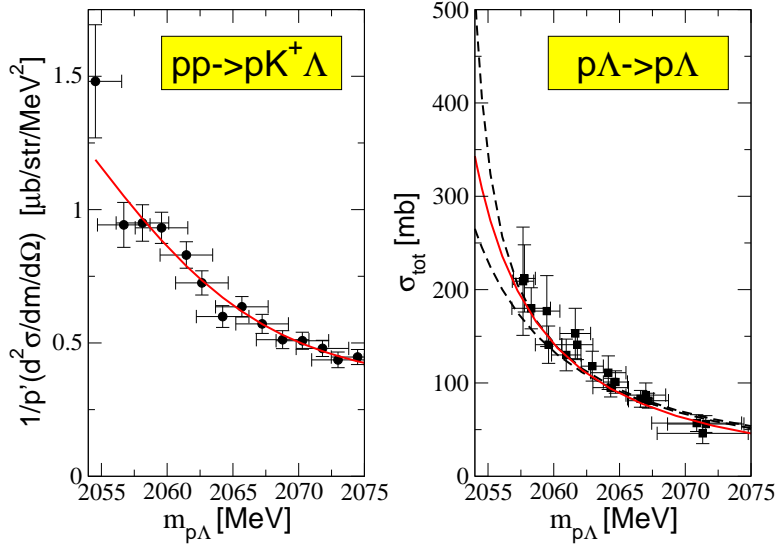


Figure 15: Illustration of the uncertainties of extraction of scattering parameters from scattering data (left panel), where an extrapolation is necessary, and from production data (right panel), where the data needs to be interpolated. The data was taken from Refs. [76, 85] for the right panel and from Ref. [86] for the left one.

reactions can be measured at COSY [61, 87] and the latter either at J-Lab [88], MAMI [89], or ELSA [90].

The essential advantages of the use of Eq. (9) to extract the scattering lengths of unstable particles compared to a determination from scattering experiments are, e.g., for  $\Lambda N$  scattering:

- Instead of an extrapolation of data, the scattering length is found from an interpolation of an invariant mass spectrum, which is theoretically much better controlled. This is illustrated in Fig. 15.
- The integral representation gives a result for the scattering length without any assumption on the energy dependence of the hyperon–nucleon interaction. This opens the possibility to fix the scattering lengths from production reactions and then use scattering data to fix, e.g., the effective range.
- Since Eq. (9) is derived from a dispersion integral, a controlled error estimate is possible. A systematic study revealed that for the kinemat-



ics relevant for the production of the  $\Lambda N$  system at low energies, the uncertainty of Eq. (9) was found to be 0.5 fm [82, 84]. Sources of this uncertainty are the possible energy dependence of the production operator, the influence of the upper limit of integration, and the possible influence of crossed channel effects.

## 10 Summary

In these proceedings various reactions on few nucleon systems were discussed. It was demonstrated that due to significant advances in the technologies of effective field theories, high precision calculations became possible for hadronic reactions even on few-nucleon systems. At the same time a clear connection to QCD is provided.

For the production of more heavy systems, like those that contain the strangeness degree of freedom, off two nucleons no effective field theory is developed yet and therefore many reactions are still being analyzed using models. However, also for this class of reactions some aspects can be analyzed in a model independent way. The  $\Lambda N$  scattering lengths were discussed as an example.

We are now in a phase, where both theory and experiment are advanced sufficiently that we should understand much better how QCD influences low energy nuclear dynamics in the upcoming years. Especially the symmetry breaking sector — violation of isospin as well as violation of the flavor  $SU(3)$  — promises deep insights into the mechanisms of strong interactions.

## Acknowledgments

I thank the organizers for a superb job and V. Lensky, V. Baru, A. Gasparyan, J. Haidenbauer, A. Kudryavtsev, and U.-G. Meißner for a very fruitful collaboration that led to the results presented.

## References

- [1] G. Colangelo, J. Gasser and H. Leutwyler, Nucl. Phys. B **603**, 125 (2001) [arXiv:hep-ph/0103088].
- [2] V. Bernard, N. Kaiser and U.-G. Meißner, Int. J. Mod. Phys. E **4** (1995) 193.

- [3] N. Fettes and U.-G. Meißner, Nucl. Phys. A **693**, 693 (2001) [arXiv:hep-ph/0101030].
- [4] B. Kubis, these proceedings.
- [5] P. F. Bedaque and U. van Kolck, Ann. Rev. Nucl. Part. Sci. **52** (2002) 339 [arXiv:nucl-th/0203055].
- [6] E. Epelbaum, Prog. Part. Nucl. Phys. **57** (2006) 654 [arXiv:nucl-th/0509032].
- [7] R. Machleidt, these proceedings.
- [8] S. Weinberg, Phys. Lett. B **295** (1992) 114.
- [9] S. R. Beane, V. Bernard, E. Epelbaum, U.-G. Meißner and D. R. Phillips, Nucl. Phys. A **720** (2003) 399. [arXiv:hep-ph/0206219].
- [10] S. R. Beane, V. Bernard, T. S. H. Lee, U.-G. Meißner and U. van Kolck, Nucl. Phys. A **618**, 381 (1997) [arXiv:hep-ph/9702226].
- [11] H. Krebs, V. Bernard and U.-G. Meißner, Eur. Phys. J. A **22** (2004) 503 [arXiv:nucl-th/0405006].
- [12] V. Baru, J. Haidenbauer, C. Hanhart and J. A. Niskanen, Eur. Phys. J. A **16**, 437 (2003) [arXiv:nucl-th/0207040].
- [13] A. Gardestig and D. R. Phillips, Phys. Rev. C **73** (2006) 014002 [arXiv:nucl-th/0501049]; A. Gardestig and D. R. Phillips, arXiv:nucl-th/0603045.
- [14] V. Lensky, V. Baru, J. Haidenbauer, C. Hanhart, A. E. Kudryavtsev and U.-G. Meißner, Eur. Phys. J. A **26**, 107 (2005) [arXiv:nucl-th/0505039].
- [15] V. Baru, C. Hanhart, A. E. Kudryavtsev and U.-G. Meißner, Phys. Lett. B **589**, 118 (2004) [arXiv:nucl-th/0402027].
- [16] B.Y. Park et al., Phys. Rev. C **53** (1996) 1519 [arXiv:nucl-th/9512023].
- [17] C. Hanhart, J. Haidenbauer, M. Hoffmann, U.-G. Meißner and J. Speth, Phys. Lett. B **424** (1998) 8 [arXiv:nucl-th/9707029].
- [18] H. Machner and J. Haidenbauer, J. Phys. G **25**, R231 (1999).
- [19] V. Dmitrašinović, K. Kubodera, F. Myhrer and T. Sato, Phys. Lett. B **465** (1999) 43 [arXiv:nucl-th/9902048].

- [20] S. I. Ando, T. S. Park and D. P. Min, Phys. Lett. B **509** (2001) 253 [arXiv:nucl-th/0003004].
- [21] T.D. Cohen, J.L. Friar, G.A. Miller and U. van Kolck, Phys. Rev. C **53** (1996) 2661 [arXiv:nucl-th/9512036].
- [22] C. da Rocha, G. Miller and U. van Kolck, Phys. Rev. C **61** (2000) 034613 [arXiv:nucl-th/9904031].
- [23] C. Hanhart, U. van Kolck, and G.A. Miller, Phys. Rev. Lett. **85** (2000) 2905 [arXiv:nucl-th/0004033].
- [24] C. Hanhart, Phys. Rep. **397** (2004) 155 [arXiv:hep-ph/0311341].
- [25] C. Hanhart and N. Kaiser, Phys. Rev. C **66** (2002) 054005 [arXiv:nucl-th/0208050].
- [26] D. R. Phillips, S. J. Wallace and N. K. Devine, Phys. Rev. C **72** (2005) 0140061. [arXiv:nucl-th/0411092].
- [27] P. Hauser *et al.*, Phys. Rev. C **58** (1998) 1869; D. Chatellard *et al.*, Nucl. Phys. A **625** (1997) 855.
- [28] D. Gotta *et al.*, PSI experiment R-06.03; D. Gotta, private communication.
- [29] S. R. Beane, V. Bernard, E. Epelbaum, U.-G. Meißner and D. R. Phillips, Nucl. Phys. A **720** (2003) 399 [arXiv:hep-ph/0206219].
- [30] U.-G. Meißner, U. Raha and A. Rusetsky, Eur. Phys. J. C **41** (2005) 213 [arXiv:nucl-th/0501073].
- [31] M. Döring, E. Oset and M. J. Vicente Vacas, Phys. Rev. C **70** (2004) 045203 [arXiv:nucl-th/0402086].
- [32] M. Pavon Valderrama and E. Ruiz Arriola, Phys. Rev. C **72** (2005) 054002 [arXiv:nucl-th/0504067]; M. P. Valderrama and E. R. Arriola, arXiv:nucl-th/0605078.
- [33] A. Nogga and C. Hanhart, Phys. Lett. B **634** (2006) 210 [arXiv:nucl-th/0511011].
- [34] L. Platter and D. R. Phillips, arXiv:nucl-th/0605024.

- [35] U.-G. Meißner, U. Raha and A. Rusetsky, Phys. Lett.B **639** (2006) 478 [arXiv:nucl-th/0512035].
- [36] A. W. Thomas and R. H. Landau, Phys. Rept. **58** (1980) 121.
- [37] B. Borasoy and H. W. Griebhammer, Int. J. of Mod. Phys. **E 12**, 65 (2003) [arXiv:nucl-th/0105048].
- [38] S. R. Beane and M. J. Savage, Nucl. Phys. A **717** (2003) 104 [arXiv:nucl-th/0204046].
- [39] M. R. Robilotta and C. Wilkin, J. Phys. G **4**, L115 (1978).
- [40] V. M. Kolybasov and A. E. Kudryavtsev, Nucl. Phys. B **41** (1972) 510.
- [41] V. Lensky, V. Baru, J. Haidenbauer, C. Hanhart, A. E. Kudryavtsev and U.-G. Meißner, Eur. Phys. J. A **26**, 107 (2005) [arXiv:nucl-th/0505039].
- [42] G. Fäldt, Phys. Scripta **16**, 81 (1977); A. Rusetsky, private communication.
- [43] J. M. Laget, Phys. Rep. **69** (1981) 1.
- [44] V. Bernard, N. Kaiser and U.-G. Meißner, Nucl. Phys. B **383** (1992) 442.
- [45] H. W. Fearing, T. R. Hemmert, R. Lewis, and C. Unkmeir, Phys. Rev. **C 62** (2000) 054006 [arXiv:hep-ph/0005213].
- [46] E. C. Booth et al., Phys. Rev. **C20** (1979) 1217.
- [47] D.E. Gonzalez–Trotter et al., Phys. Rev. Lett. **83** (1999) 3788; V. Huhn et al., Phys. Rev. Lett. **85** (2000) 1190.
- [48] C. Hanhart and A. Wirzba, arXiv:nucl-th/0703012.
- [49] A. Gårdestig, talk presented at ECT\* workshop 'Charge Symmetry Breaking and Other Isospin Violations', Trento, June 2005; A. Gårdestig, D. R. Phillips and C. Elster, arXiv:nucl-th/0511042.
- [50] V. Lensky, V. Baru, J. Haidenbauer, C. Hanhart, A. E. Kudryavtsev and U.-G. Meißner, Eur. Phys. J. A **27**, 37 (2006) [arXiv:nucl-th/0511054].
- [51] D. Koltun and A. Reitan, Phys. Rev. **141** (1966) 1413.
- [52] D. A. Hutcheon *et al.*, Nucl. Phys. A **535** (1991) 618.

- [53] P. Heimberg *et al.*, Phys. Rev. Lett. **77** (1996) 1012.
- [54] M. Drochner *et al.*, Nucl. Phys. A **643** (1998) 55.
- [55] J. A. Niskanen, Phys. Rev. C **53**, 526 (1996) [arXiv:nucl-th/9502015].
- [56] C. Hanhart, J. Haidenbauer, O. Krehl and J. Speth, Phys. Lett. B **444** (1998) 25 [arXiv:nucl-th/9808020].
- [57] C. Hanhart, J. Haidenbauer, O. Krehl and J. Speth, Phys. Rev. C **61** (2000) 064008 [arXiv:nucl-th/0002025].
- [58] B. von Przewoski *et al.*, Phys. Rev. C **61** (2000) 064604.
- [59] W. W. Daehnick *et al.*, Phys. Rev. C **65** (2002) 024003.
- [60] H. O. Meyer *et al.*, Phys. Rev. C **63** (2001) 064002.
- [61] A. Kacharava *et al.*, arXiv:nucl-ex/0511028.
- [62] V. C. Highland *et al.*, Nucl. Phys. A **365** (1981) 333.
- [63] K. Brückner, Phys. Rev. **98** (1955) 769.
- [64] I.R. Afnan and A.W. Thomas, Phys. Rev. C **10** (1974) 109; D.S. Koltun and T. Mizutani, Ann. Phys. (N.Y.) **109** (1978) 1.
- [65] T. E. O. Ericson, B. Loiseau, A. W. Thomas, Phys. Rev. C **66** (2002) 014005 [arXiv:hep-ph/0009312].
- [66] V. Baru, A. Kudryavtsev, Phys. Atom. Nucl., **60** (1997) 1476.
- [67] V. Lensky, V. Baru, J. Haidenbauer, C. Hanhart, A. E. Kudryavtsev and U.-G. Meißner, arXiv:nucl-th/0608042; Phys. Lett. B, in print.
- [68] R. Machleidt, Phys. Rev. C **63** (2001) 024001 [arXiv:nucl-th/0006014].
- [69] A. K. Opper *et al.*, Phys. Rev. Lett. **91** (2003) 212302 [arXiv:nucl-ex/0306027].
- [70] E. J. Stephenson *et al.*, Phys. Rev. Lett. **91** (2003) 142302 [arXiv:nucl-ex/0305032].
- [71] U. van Kolck, J. A. Niskanen, and G. A. Miller, Phys. Lett. B **493** (2000) 65 [arXiv:nucl-th/0006042].

- [72] A. Gårdestig *et al.*, Phys. Rev. C **69** (2004) 044606[arXiv:nucl-th/0402021].
- [73] A. Nogga *et al.*, Phys. Lett. B **639**, 465 (2006) [arXiv:nucl-th/0602003].
- [74] A. Bernstein, private communication.
- [75] G. Alexander *et al.*, Phys. Lett. **19**, 715 (1966); B. Sechi-Zorn *et al.*, Phys. Rev. **175**, 1735 (1968).
- [76] G. Alexander *et al.*, Phys. Rev. **173**, 1452 (1968);
- [77] T. A. Rijken, V. G. J. Stoks, Y. Yamamoto, Phys. Rev. C **59** (1999) 21.
- [78] J. Haidenbauer, U.-G. Meißner, Phys. Rev. C **72** (2005) 044005.
- [79] H. Polinder, J. Haidenbauer and U. G. Meissner, Nucl. Phys. A **779** (2006) 244 [arXiv:nucl-th/0605050]; J. Haidenbauer, U. G. Meissner, A. Nogga and H. Polinder, arXiv:nucl-th/0702015.
- [80] C. Hanhart, arXiv:hep-ph/0609136.
- [81] N. I. Muskhelishvili, *Singular Integral Equations*, (P. Noordhof N. V., Groningen, 1953); R. Omnes, Nuovo Cim. **8**, 316 (1958); W. R. Frazer and J. R. Fulco, Phys. Rev. Lett. **2**, 365 (1959).
- [82] A. Gasparyan, J. Haidenbauer, C. Hanhart and J. Speth, Phys. Rev. C **69**, 034006 (2004) [arXiv:hep-ph/0311116].
- [83] A. Gasparyan, J. Haidenbauer and C. Hanhart, Phys. Rev. C **72**, 034006 (2005) [arXiv:nucl-th/0506067].
- [84] A. Gasparyan, J. Haidenbauer, C. Hanhart and K. Miyagawa, arXiv:nucl-th/0701090.
- [85] F. Eisele *et al.* Phys. Lett. B **37**, 1971 (204).
- [86] R. Siebert *et al.*, Nucl. Phys. **A567**, 819 (1994).
- [87] A. Gillizer *et al.*, in preparation.
- [88] B.L. Berman *et al.*, CEBAF proposal PR-89-045 (1989).
- [89] R. Beck and A. Starostin, Eur. Phys. J. A **S19**, 279 (2004); R. Beck, Prog. Part. Nucl. Phys. **55**, 91 (2005).
- [90] V. Kleber and H. Schmieden, private communication.